1  # Human Endometrial Stromal Cells Are Highly Permissive To Productive

2  # Infection by Zika Virus

3

4  Isabel Pagani[1,9], Silvia Ghezzi[1,9], Adele Ulisse[2], Alicia Rubio[3], Filippo Turrini[1],

5  Elisabetta Garavaglia[4], Massimo Candiani[4,5], Concetta Castilletti[6], Giuseppe Ippolito[6],

6  Guido Poli[5,7], Vania Broccoli[8], Paola Panina-Bordignon[2,10*] and Elisa Vicenzi[1,10*]

7

8  [1]Viral Pathogens and Biosafety Unit, Division of Immunology, Transplantation and

9  Infectious Diseases, San Raffaele Scientific Institute, Milan, Italy;

10  [2]Reproductive Sciences Laboratory, Division of Genetics and Cell Biology, San Raffaele

11  Scientific Institute, Milan, Italy;

12  [3]Division of Neuroscience, San Raffaele Scientific Institute, Milan, Italy;

13  [4]Obstetrics and Gynecology Unit, San Raffaele Scientific Institute, Milan, Italy;

14  [5]Vita-Salute San Raffaele University School of Medicine, Milan, Italy.

15  [6]National Institute for Infectious Diseases "Lazzaro Spallanzani", Rome, Italy;

16  [7]AIDS Immunopathogenesis Unit, Division of Immunology, Transplantation and

17  Infectious Diseases, San Raffaele Scientific Institute, Milan, Italy;

18  [8]National Research Council (CNR), Institute of Neuroscience, Milan, Italy;

19

20  [9]co-first authors; [10]co-last authors

21  *Correspondence: panina.paola@hsr.it (P.P.-B.), vicenzi.elisa@hsr.it (E.V.)

22

23  Short title: Zika virus infection of human endometrium.

24

25 **ABSTRACT**

26      Zika virus (ZIKV) is a recently re-emerged flavivirus transmitted to humans by

27 mosquito bites but also from mother to fetus and by sexual intercourse. We here show for

28 the first time that primary human endometrial stromal cells (HESC) are highly permissive

29 to ZIKV infection and support its *in vitro* replication. ZIKV envelope expression was

30 detected in the endoplasmic reticulum whereas double-stranded viral RNA colocalized

31 with vimentin filaments to the perinuclear region. ZIKV productive infection also

32 occurred in the human T-HESC cell line with the induction of interferon-β (IFN-β) and of

33 IFN-stimulated genes. Notably, *in vitro* decidualization of T-HESC with cyclic AMP and

34 progesterone upregulated the cell surface expression of the ZIKV entry co-receptor AXL

35 and boosted ZIKV replication by *ca.* 100-fold. Thus, endometrial stromal cells,

36 particularly if decidualized, likely represent a crucial cell target of sexual virus

37 transmission and a relevant source of ZIKV spreading to placental trophoblasts during

38 pregnancy.

39

40 **Key words:** ZIKV, endometrial cells, AXL, IFN-β, sexual transmission

41    **AUTHOR SUMMARY**

42        Infection by Zika virus (ZIKV), a flavivirus transmitted to humans by mosquito

43    bites, has recently emerged as an important cause of neurological lesions in the fetal brain

44    as women who become infected by ZIKV during pregnancy can transmit the virus to their

45    fetus. In addition, routes of ZIKV transmission independent of mosquito bites  have been

46    also identified and include sexual transmission from both infected men and women to

47    their partners, an aspect bearing great societal implications for ZIKV spread. These

48    observations highlight the importance of the female reproductive tract in the

49    establishment and/or spreading of the infection. In this regard, the endometrium is a

50    highly dynamic tissue undergoing major histological changes during the menstrual cycle

51    under the coordinated action of sexual hormones. In particular, progesterone drives the

52    differentiation of human endometrial stromal cells towards decidualization, a process that

53    is critical for fetal trophoblast invasion and placenta formation. We here report for the

54    first time that both primary and immortalized human endometrial stromal cells are highly

55    permissive to ZIKV infection and replication, particularly when *in vitro* decidualized by

56    progesterone, suggesting that these cells could significantly contribute to vertical ZIKV

57    transmission in utero during pregnancy but also to horizontal transmission by the sexual

58    route.

59 **INTRODUCTION**

60      Zika Virus (ZIKV) is a member of the *Flaviviridae* family transmitted to humans

61 by mosquito bites of the *Aedes* species [1]. The virus has been first isolated from the

62 blood of a febrile monkey in 1947 in the Zika forest of Uganda [2]; however, its potential

63 as a human pathogen was underestimated for almost 60 years until 2013 when an unsual

64 outbreak of ZIKV-related Guillain-Barré syndrome emerged in French Polynesia [3]. A

65 global health emergency was triggered at the end of 2015 by the obervation of an

66 increased incidence of microcephaly was associated with the temporal and geographic

67 distribution of ZIKV infection in the North East Brazil [4]. Increasing evidence now

68 clearly supports a cause-effect relationship between congenital ZIKV transmission and

69 increased frequency of mild to severe neuropathologies including microcephaly [5,6].

70 ZIKV was detected in the amniotic fluid of pregnant women [7] suggesting that the

71 placenta might be permissive to virus passage, a condition that likely occurs during the

72 first trimester of pregnancy [8], although placental cells appear to be protected against

73 ZIKV infection by a constitutive interferon (IFN)-$\lambda$1 response [9]. Indeed, two recent

74 studies showed that human primary placental macrophages and trophoblasts were

75 permissive to ZIKV productive infection both *in vitro* [10,11] and in a mice [12]. These

76 studies demonstrates that ZIKV can cross the placental barrier either coming from

77 maternal blood or by an ascending route as recently demonstrated in a mouse model of

78 vaginal ZIKV infection [13].

79      Vector-independent transmission of ZIKV among humans can occur through the

80 sexual route [14]. Male-to-female transmission has been reported in approximately 15

81 cases thus far [15]. This hypothesis is also supported by both the detection of higher viral

82    load in semen *vs.* blood and by the persistence of ZIKV in semen for several months after

83    waning of symptoms [16,17,18,19]. More recently, female-to-male sexual transmission of

84    ZIKV infection was also documented [20]. These observations imply a potentially

85    prominent role of the female reproductive tract (FRT) as a site of virus infection and

86    propagation either from and to the male partner during sexual intercourse or to the fetus

87    during pregnancy. All compartments of the FRT, including the endometrium, might

88    contribute to establishing and spreading the initial infection. In addition, it should be

89    taken into consideration the fact that the human endometrium is a highly dynamic tissue

90    undergoing major histological changes during the menstrual cycle under the coordinated

91    action of sexual hormones. Estrogen dominates the proliferative phase of the menstrual

92    cycle, while the post-ovulatory rise of ovarian progesterone drives the differentiation of

93    human endometrial stromal cells (HESC). This process, known as pre-decidualization, is

94    critical for fetal trophoblast invasion and placenta formation and occurs independently of

95    an implanting blastocyst [21].

96         Therefore, we investigated whether primary HESC or immortalized (T-HESC)

97    cells were permissive to *in vitro* ZIKV infection and replication. Indeed, ZIKV

98    productively infected both HESC and T-HESC, whereas *in vitro* decidualization of the

99    cell line (dT-HESC) increased both the expression of putative ZIKV entry co-receptor

100   AXL and the levels of productive infection *vs.* unstimulated cells. Thus, our results fully

101   support the hypothesis of a relevant role of the endometrium for both sexual ZIKV

102   transmission and *in utero* virus transmission to the fetus during pregnancy.

103 **RESULTS**

104 ***ZIKV infection of primary HESC.*** Primary HESC were isolated from

105 endometrial biopsies and incubated with either the reference African MR766 or

106 contemporary INMI-1 strains at the multiplicity of infection (MOI) of 10 after reaching

107 cell confluency (days 3-4). Viral growth was firstly analyzed by indirect

108 immunofluorescence (IF) analysis using either an anti-dsRNA monoclonal antibody

109 (mAb) or an anti-panflavivirus envelope (E) protein mAb. Subcellular distributions of

110 both viral RNA and E protein were observed 72 h after infection of HESC (**Figure 1A**).

111 The percentage of cells infected with the MR766 strain, as measured by both anti-dsRNA

112 and anti-flavi E mAb staining, was *ca.* 80% whereas the proportion of cells infected with

113 the INMI-1 strain was 10-fold lower (ca. 7%). Progeny infectious virion production was

114 measured in HESC culture supernatants using a standard plaque-forming assay (PFA) in

115 Vero cells (**Figure 1B**) whereas absolute quantification of viral NS5 RNA was

116 determined by droplet digital (dd) PCR (**Figure 1C**). Both viral strains replicated

117 efficiently in primary HESC established from 8 independent donors although the more

118 recent INMI-1 strain was *ca.* 1 $\log_{10}$ less efficient than the MR766 strain, confirming the

119 IF results.

120 ***Subcellular localization of ZIKV in HESC.*** The flavivirus life cycle occurs in the

121 cytoplasm mostly in association with intracellular membranes of the endoplasmic

122 reticulum (ER) [22]. Therefore, we analyzed whether ZIKV E protein co-localized with

123 the ER in infected cells by staining infected and uninfected cells with a mAb directed to

124 calreticulin, a major $Ca^{2+}$-binding protein and chaperone expressed in the lumen of the

125 ER [23]. Calreticulin staining in uninfected cells appeared as perinuclear fibrillar

126    fluorescence (**Figure 2A**) whereas in infected cells its staining expanded in the cytoplasm

127    towards the cell perifery. In addition, dense structures colocalized viral E protein

128    expression and calreticulin in the perinuclear region (**Figure 2A**).

129         We also evaluated whether vimentin, a major component of type III intermediate

130    filaments expressed by HESC [24], colocalized with ZIKV dsRNA. It has been reported

131    previously that vimentin filaments are redistributed during cell infection with Dengue

132    virus (DENV) as they are essential for the anchorage of the virus replication complex

133    [25]. In uninfected HESC vimentin displayed a tipically extended network arrangement

134    from the perinuclear region outwards to the cell plasma membrane (**Figure 2B**). Of note

135    is the fact that ZIKV infection induced retraction of vimentin filaments from the cell

136    periphery and their reorganization into dense structures in the perinuclear region (**Figure

137    2B**). Viral dsRNA IF showed a punctate structure that indeed co-localized with vimentin

138    dense structures (**Figure 2B**).

139         Productive infection of two additional ZIKV strains, Puerto Rican 2015

140    (PRVABC59) and Thailand 2013 [26], was observed in primary HESC by both PFA and

141    ddPCR of viral RNA (**Figure S1A** and **B,** respectively) 3 days post-infection, confirming

142    intracellular co-localization of the E protein and dsRNA with calreticulin and vimentin,

143    respectively (**Figure S1C** and **D**).

144         Thus, primary HESC are targets of *in vitro* infection and actively support the

145    replication of different ZIKV strains in the ER and in association with vimentin

146    filaments.

147         **In vitro *decidualization of T-HESC cells upregulates ZIKV productive***

148    ***infection.*** In order to test whether decidualization could influence ZIKV infection, we

149  infected the immortalized T-HESC cell line either in unstimulated conditions or

150  following *in vitro* decidualization induced by progesterone and cAMP, as reported [27].

151  As shown by IF with both anti-dsRNA and anti-E protein mAbs, the MR766 strain

152  productively infected T-HESC. A significant increase of the percentage of infected cells

153  of *ca.* 2-fold was observed by IF staining of dT-HESC vs. control cells (**Figure 3A**).

154      The expression of two putative entry co-receptors for ZIKV entry, AXL and

155  MER, was evaluated by cytofluorimetric analysis in both uninfected T-HESC and dT-

156  HESC. While MER expression was not detectable, AXL was expressed by unstimulated

157  T-HESC and, of note, it was upregulated in dT-HESC (RFI: 2.76 vs. 1.64, respectively;

158  **Figure 3B**), consistently with the higher infection efficiency observed in these

159  experimental conditions.

160      As observed with primary cells, calreticulin staining in uninfected cells appeared

161  as a perinuclear fibrillar fluorescence whereas it expanded in the cytoplasm towards the

162  cell perifery and colocalized with viral E protein expression in infected cells (**Figure 3C**).

163  Punctate structures were observed in infected dT-HESCs stained with an anti-dsRNA Ab

164  that colocalized with vimentin filaments in the perinuclear region (**Figure 3D**).

165      ***ZIKV productive infection of T-HESC is cytopathic and induces the expression***

166  ***of IFN-$\beta$ and ISGs.*** By PFA we next determined the kinetics of virus replication in T-

167  HESC and dT-HESC cells by analyzing their culture supernatants in Vero cells. Virus

168  replication in T-HESC of both MR766 and INMI-1 strains increased by approximately

169  10- and 5-fold over the levels of input virus, respectively, peaking around 96 h post-

170  infection (**Figure 4A, left panel**). Decidualization of T-HESC increased the efficiency of

171  virus replication by up to two orders of magnitude after 144 h post-infection (**Figure 4A,**

172    **right panel**). Peak virus replication was detected by ddPCR 96 h post-infection and

173    levels *ca.* 10 fold higher than those of the input virus were maintained up to 144 h post-

174    infection (**Figure 4B**). ZIKV infection of both untreated T-HESC and dT-HESC induced

175    cytopathicity and cell death as determined by the levels of adenylate kinase (AK)

176    released in the culture supernatants [28] with kinetics overlapping those of virus

177    replication (**Figure 4C**).

178         Since it has been reported that ZIKV infection leads to the transcription and

179    release of IFN-β in human skin fibroblasts [29], we evaluated the kinetic of IFN-β mRNA

180    expression by RT-qPCR after infection of T-HESC. Indeed, higher levels of IFN-β gene

181    transcription were detected 24 h after infection vs. those of uninfected cells and increased

182    of ca. 300-fold 6 days after infection of T-HESC with the MR766 strain, whereas lower

183    levels were induced upon infection with the INMI-1 strain (**Figure 4D**). The virus-

184    induced levels of IFN-β mRNA in dT-HESC cells were similar to those of T-HESC cells;

185    however, a more rapid insurgence of IFN- β expression was observed in T-HESC vs. dT-

186    HESC (**Figure 4D**).

187         We next determined whether biologically active IFN-β was indeed secreted

188    following ZIKV infection of T-HESC and dT-HESC cells. For this purpose, cell culture

189    supernatants were tested on HEK-Blue IFN-α/β cells containing the secreted alkaline

190    phosphatase (SEAP) reporter gene under the control of IFN-α/β inducible ISG54

191    promoter [30]. The induction of SEAP activity confirmed the presence of bioactive type 1

192    IFN in the supernatants of infected cells with moderately delayed kinetics in comparison

193    to the upregulation of IFN-β mRNA observed in infected cells (**Figure S2**).

194        Among ISGs, myxovirus resistance protein 1 (MXA) and 2'-5'-Oligoadenylate

195    Synthetase (OAS2) were previously shown to be genes that were mostly upregulated by

196    ZIKV infection of fibroblasts [29]; therefore, we determined their kinetics of expression

197    by RT-PCR. Both MXA and OAS2 mRNAs were upregulated in ZIKV infected vs.

198    uninfected cells (**Figure 4E** and **F**, respectively) with kinetics almost superimposable to

199    those of IFN-β mRNA expression; no quantitative differences were observed for these

200    ISGs in cells infected with the MR766 and INMI-1 strains, in spite of different levels of

201    virus replication.

202

203 **DISCUSSION**

204      In the present study, we report for the first time that primary HESC are highly

205 permissive to ZIKV productive infection by both an historic and different contemporary

206 strains. We also showed that the T-HESC cell line, which models HESC in the

207 proliferative phase, was permissive to ZIKV infection and supported virus replication.

208 Infection of T-HESC strongly upregulated the expression of bioactive IFN-β and of

209 related ISGs (MXA, OAS2). Interestingly, *in vitro* decidualization of T-HESC, increased

210 the efficiency of ZIKV replication by up to 100-fold in association with the upregulation

211 of the putative entry co-receptor AXL, but not of MER, suggesting a potential correlate

212 of the increased levels of virus replication observed upon decidualization of the cell line.

213      Flaviviruses bind to a variety of surface molecules that serve as entry mediators or

214 cofactors including the TAM family of tyrosine kinase receptors [31]. Among TAMs,

215 AXL was reported to mediate ZIKV entry in dermal fibroblasts and epidermal

216 keratinocytes [29]. Furthermore, AXL is highly expressed by neural stem cells, a

217 privileged target of ZIKV infection in the fetal central nervous system [32] whereas it

218 might play a minor role as compared with other TAM entry factors in placental cells [33].

219 Of importance is the observation that AXL was confirmed as ZIKV entry factor in a

220 CRISPR/Cas9 screen of HeLa cells [34]. Our results support the hypothesis of a

221 prominent role of AXL in infection of HESC and a potential deleterious role of

222 progesterone in favoring virus transmission to the trophoblasts, in case of pregnancy, or

223 from and to a male partner during sexual intercourse.

224      As for DENV, we observed that ZIKV dsRNA associated with vimentin

225 intermediate filaments that were rearranged in the perinuclear region of infected HESC

226    and T-HESC [25]. This observation suggests a potential role of vimentin in ZIKV RNA

227    amplification machinery, perhaps by stabilization of replication complexes, as suggested

228    for DENV replication [25]. We also observed that ZIKV E protein was localized in the

229    ER of infected HESC and T-HESC cells, which showed dilated *cisternae* as a sign of

230    massive expansion of the cell secretory machinery. These observations indicate that

231    ZIKV, similarly to DENV, assembles and accumulates its progeny virions in the ER sacs

232    [35] where a subset of ER-associated signal peptidase complex proteins is responsible for

233    the proper cleavage of flavivirus structural proteins and secretion of viral particles [36].

234    The kinetics of ZIKV replication well correlated with the production of active IFN-β and

235    the consequent induction of ISGs, such as MXA and OAS2, that likely curtailed

236    spreading of infection.

237          Very recently, ZIKV has been detected in the FRT after the onset of clinical

238    symptoms [37] and both male-to-female [15,38] and female-to-male transmission [20]

239    have been documented suggesting that this vector-independent route of viral transmission

240    might have occurred more frequently than reported. Furthermore, ZIKV presence in the

241    FRT can foster vertical transmission from mother to fetus, as recently demonstrated in a

242    mouse model of vaginal virus infection [13] and previously demonstrated for other

243    members of the *Flaviviridae* family such as hepatitis C virus, in which vertical

244    transmission from mother to child can occur in up to 10% of pregnancies [37]. As

245    maternal decidual cells are in direct contact with extravillous trophoblast (EVT) on the

246    tip of anchoring villi, one possibility is that ZIKV produced by infected HESC and/or

247    other cells present in the FRT is transmitted to EVT in early pregnancy and then enters

248    the fetal circulation.

249     An unclear aspect of ZIKV pathogenesis is whether ZIKV infection persists for

250     longer in spite of its cytopathicity. If this is the case, ZIKV persistence in decidualized

251     HESC might provide a viral reservoir for infection of cells of the *decidua basalis*, thus

252     favoring viral transmission to chorionic villi.

253     Although ZIKV transmission occurs primarily through *Aedes* mosquitos bites,

254     increasing evidence of vector-independent viral transmission through the sexual route

255     bear potentially great societal implications for ZIKV spread [15]. Our *in vitro* findings

256     indicate a vulnerability of the FRT to ZIKV infection, particularly upon endometrial

257     decidualization by progesterone, as previously observed for other sexually transmitted

258     viruses, such as herpes simplex virus and HIV [39]. As for these virus, topical

259     microbicides developed and formulated for vaginal use [40] should be considered among

260     the preventative strategies against ZIKV infection.

261 **METHODS**

262     *Human Tissues*. Endometrial biopsies from 7 pre-menopausal women with regular

263 menstrual cycles (5 in proliferative phase and 2 in secretory phase) and from 1 peri-

264 menopause woman, all undergoing histeroscopy for diagnostic purposes, were obtained

265 from the Ob&Gyn Department of the San Raffaele Scientific Institute in Milan. The

266 selected women did not show any evident endometrial pathology or suffer from any

267 endocrine disorder or systemic disease and have not received any steroid treatment for at

268 least 3 months prior to tissue collection. Uterine samples were obtained by Vacuum

269 Aspiration Biopsy Random Assay (Vabra). All women provided written informed

270 consent before tissue collection and anonymized samples were delivered to the laboratory

271 (see **Supporting Information** for the details of tissue culture preparation).

272     The immortalized human endometrial stromal cell line T-HESC, originated from

273 normal human endometrial stromal cell immortalized with hTERT (Krikun et al, 2004),

274 was obtained from ATCC (CRL-4003™). Cells were maintained in complete growth

275 medium according to the manufacturer's instructions. To induce T-HESC cell

276 decidualization, stromal cells were stimulated with cAMP (0.5 mM; Sigma) and

277 medroxyprogesterone acetate (MPA) (1 μM; Sigma) for 7 days.

278     ***ZIKV infection.*** The viral strain MR766 was obtained  from the European virus

279 archive (EVAg) and expanded in Vero cells. The Brazilian 2016/INMI-1 isolate

280 (GenBank Accession # KU991811) was obtained from an Italian individual who traveled

281 to Brazil in January 2016. HESC or T-HESC cells were seeded in 24 well plastic plates at

282 $2.5 \times 10^5$/ml; cell culture medium was removed from confluent cells and was replaced with

283 virus containing supernatant at the MOI of 10. After 4 h, the supernatant was removed

284    and fresh culture medium (0.5 ml) was added. The kinetics of virus replication were

285    measured in supernatants collected 1, 24, 72 and 144 h post-infection and kept frozen at -

286    80°C until further use (see **Supporting Information**).

287        ***Indirect immunofluorescence of ZIKV E protein and dsRNA***. Cells were fixed

288    for 20 min in 4% paraformaldehyde solution (Sigma) in phosphate-buffered saline (PBS,

289    Euroclone). Cells were permeabilized for 30 min in blocking solution, containing 0.2%

290    Triton X-100 (Sigma) and 10% donkey serum (Sigma) and incubated overnight at 4°C

291    with the primary mAb in blocking solution. The following mAbs specific for Flavivirus E

292    protein (1:200, Millipore, MAB10216), double-stranded RNA (1:300, English and

293    Scientific Consulting Kft, Hungary), vimentin (1:300, Bioss, BS-0756R) and calreticulin

294    (1:300, Sigma, C4606) were used. Cells were then washed with PBS and incubated for 1h

295    with Hoechst and either anti-mouse Alexa Fluor-488 or anti-rabbit Alexa Fluor-594

296    secondary Abs (1:1,000 in blocking solution, ThermoFisher Scientific). After PBS

297    washes, cells were washed again and mounted.

298        ***Flow Cytometry.*** Mouse anti-human AXL mAb (clone # 108724, MAB154) and

299    mouse anti-human MER mAb (clone # 125518, MAB8912) was purchased from R&D

300    Systems. Goat anti-mouse IgG secondary antibody, RPE conjugated was purchased from

301    ThermoFisher Scientific (P-852). $2 \times 10^4$ T-HESC were used per condition. Samples were

302    acquired on FACSCanto (BD) flow cytometer. Dead cells were excluded on the basis of

303    propidium iodide and DAPI staining. All data were analyzed using FlowJo software

304    (Tree Star). Relative fluorescent intensity (RFI) of AXL and MER expression on T-

305    HESC was calculated dividing the mean AXL and MER fluorescence intensity by the

306    mean fluorescence intensity of the corresponding isotype control mAb.

307       ***Cell death detection assay.*** 10 μl samples of culture supernatant were transferred

308       on a half black 96 well plate (Costar). To each well, 50 μl of the adenylate kinase

309       detection reagent (ToxiLight® BioAssay, Lonza) was added and the plate was incubated

310       for 10 min at room temperature. Luminescence was measured in a Mithras LB940

311       Microplate Reader (Berthold Technologies). The results were expressed as relative

312       luminescent unit (RLU).

313       ***RT-qPCR for IFN-$\beta$ and ISGs.*** Total RNA was extracted from either non-

314       decidualized or decidualized T-HESC cells by using a TRIzol Plus RNA purification kit,

315       followed by DNase I treatment (Invitrogen). cDNA was synthesized from total RNA (1

316       μg) using a SuperScript first-strand synthesis system (Invitrogen) with random hexamers.

317       SYBR green (Applied Biosystems) qPCR was performed with 50 ng of cDNA in a total

318       volume of 25 µl with the primer pair (250 nM) described in the **Table S1**. All reactions

319       were performed with an ABI 7700 Prism instrument (Applied Biosystems). mRNA

320       expression was calculated by using the relative quantification method to uninfected

321       samples after normalized to human glyceraldehyde-3-phosphate dehydrogenase

322       (GAPDH) mRNA expression.

323       ***Statistical Analysis.*** Prism GraphPad software v. 4.0 (www.graphpad.com) was

324       used for all statistical analyses. Comparison between two groups was performed using the

325       Student's t-test.

## ACKNOWLEDGMENTS

**REFERENCES**

1. Musso D, Gubler DJ (2016) Zika Virus. Clinical microbiology reviews 29: 487-524.
2. Dick GW, Kitchen SF, Haddow AJ (1952) Zika virus. I. Isolations and serological specificity. Transactions of the Royal Society of Tropical Medicine and Hygiene 46: 509-520.
3. Cao-Lormeau VM, Blake A, Mons S, Lastere S, Roche C, et al. (2016) Guillain-Barre Syndrome outbreak associated with Zika virus infection in French Polynesia: a case-control study. Lancet 387: 1531-1539.
4. Besnard M, Eyrolle-Guignot D, Guillemette-Artur P, Lastere S, Bost-Bezeaud F, et al. (2016) Congenital cerebral malformations and dysfunction in fetuses and newborns following the 2013 to 2014 Zika virus epidemic in French Polynesia. Euro surveillance : bulletin Europeen sur les maladies transmissibles = European communicable disease bulletin 21.
5. Brasil P, Pereira JP, Jr., Raja Gabaglia C, Damasceno L, Wakimoto M, et al. (2016) Zika Virus Infection in Pregnant Women in Rio de Janeiro - Preliminary Report. The New England journal of medicine.
6. Driggers RW, Ho CY, Korhonen EM, Kuivanen S, Jaaskelainen AJ, et al. (2016) Zika Virus Infection with Prolonged Maternal Viremia and Fetal Brain Abnormalities. The New England journal of medicine.
7. Calvet G, Aguiar RS, Melo AS, Sampaio SA, de Filippis I, et al. (2016) Detection and sequencing of Zika virus from amniotic fluid of fetuses with microcephaly in Brazil: a case study. The Lancet Infectious diseases.
8. Adibi JJ, Marques ET, Jr., Cartus A, Beigi RH (2016) Teratogenic effects of the Zika virus and the role of the placenta. Lancet 387: 1587-1590.
9. Bayer A, Lennemann NJ, Ouyang Y, Bramley JC, Morosky S, et al. (2016) Type III Interferons Produced by Human Placental Trophoblasts Confer Protection against Zika Virus Infection. Cell host & microbe 19: 705-712.
10. Quicke KM, Bowen JR, Johnson EL, McDonald CE, Ma H, et al. (2016) Zika Virus Infects Human Placental Macrophages. Cell host & microbe 20: 83-90.
11. Tabata T, Petitt M, Puerta-Guardo H, Michlmayr D, Wang C, et al. (2016) Zika Virus Targets Different Primary Human Placental Cells, Suggesting Two Routes for Vertical Transmission. Cell host & microbe.
12. Miner JJ, Cao B, Govero J, Smith AM, Fernandez E, et al. (2016) Zika Virus Infection during Pregnancy in Mice Causes Placental Damage and Fetal Demise. Cell 165: 1081-1091.
13. Yockey LJ, Varela L, Rakib T, Khoury-Hanold W, Fink SL, et al. (2016) Vaginal Exposure to Zika Virus during Pregnancy Leads to Fetal Brain Infection. Cell.
14. D'Ortenzio E, Matheron S, Yazdanpanah Y, de Lamballerie X, Hubert B, et al. (2016) Evidence of Sexual Transmission of Zika Virus. The New England journal of medicine 374: 2195-2198.
15. Grischott F, Puhan M, Hatz C, Schlagenhauf P (2016) Non-vector-borne transmission of Zika virus: A systematic review. Travel Medicine and Infectious Disease.
16. Nicastri E, Castilletti C, Liuzzi G, Iannetta M, Capobianchi MR, et al. (2016) Persistent detection of Zika virus RNA in semen for six months after symptom onset in a traveller returning from Haiti to Italy, February 2016. Euro surveillance

375      : bulletin Europeen sur les maladies transmissibles = European communicable
376      disease bulletin 21.

377  17. Atkinson B, Hearn P, Afrough B, Lumley S, Carter D, et al. (2016) Detection of Zika
378      Virus in Semen. Emerging infectious diseases 22: 940.

379  18. Musso D, Roche C, Robin E, Nhan T, Teissier A, et al. (2015) Potential sexual
380      transmission of Zika virus. Emerging infectious diseases 21: 359-361.

381  19. Mansuy JM, Pasquier C, Daudin M, Chapuy-Regaud S, Moinard N, et al. (2016) Zika
382      virus in semen of a patient returning from a non-epidemic area. The Lancet
383      Infectious diseases 16: 894-895.

384  20. Davidson A, Slavinski S, Komoto K, Rakeman J, Weiss D (2016) Suspected Female-
385      to-Male Sexual Transmission of Zika Virus - New York City, 2016. MMWR
386      Morbidity and mortality weekly report 65: 716-717.

387  21. Brosens JJ, Gellersen B (2006) Death or survival--progesterone-dependent cell fate
388      decisions in the human endometrial stroma. Journal of molecular endocrinology
389      36: 389-398.

390  22. Blazquez AB, Escribano-Romero E, Merino-Ramos T, Saiz JC, Martin-Acebes MA
391      (2014) Stress responses in flavivirus-infected cells: activation of unfolded protein
392      response and autophagy. Frontiers in microbiology 5: 266.

393  23. Aebi M, Bernasconi R, Clerc S, Molinari M (2010) N-glycan structures: recognition
394      and processing in the ER. Trends in biochemical sciences 35: 74-82.

395  24. Osteen KG, Hill GA, Hargrove JT, Gorstein F (1989) Development of a method to
396      isolate and culture highly purified populations of stromal and epithelial cells from
397      human endometrial biopsy specimens. Fertility and sterility 52: 965-972.

398  25. Teo CS, Chu JJ (2014) Cellular vimentin regulates construction of dengue virus
399      replication complexes through interaction with NS4A protein. Journal of virology
400      88: 1897-1913.

401  26. Fonseca K, Meatherall B, Zarra D, Drebot M, MacDonald J, et al. (2014) First case of
402      Zika virus infection in a returning Canadian traveler. The American journal of
403      tropical medicine and hygiene 91: 1035-1038.

404  27. Krikun G, Mor G, Alvero A, Guller S, Schatz F, et al. (2004) A novel immortalized
405      human endometrial stromal cell line with normal progestational response.
406      Endocrinology 145: 2291-2296.

407  28. Single B, Leist M, Nicotera P (1998) Simultaneous release of adenylate kinase and
408      cytochrome c in cell death. Cell death and differentiation 5: 1001-1003.

409  29. Hamel R, Dejarnac O, Wichit S, Ekchariyawat P, Neyret A, et al. (2015) Biology of
410      Zika Virus Infection in Human Skin Cells. Journal of virology 89: 8880-8896.

411  30. Frumence E, Roche M, Krejbich-Trotot P, El-Kalamouni C, Nativel B, et al. (2016)
412      The South Pacific epidemic strain of Zika virus replicates efficiently in human
413      epithelial A549 cells leading to IFN-beta production and apoptosis induction.
414      Virology 493: 217-226.

415  31. Perera-Lecoin M, Meertens L, Carnec X, Amara A (2014) Flavivirus entry receptors:
416      an update. Viruses 6: 69-88.

417  32. Nowakowski TJ, Pollen AA, Di Lullo E, Sandoval-Espinosa C, Bershteyn M, et al.
418      (2016) Expression Analysis Highlights AXL as a Candidate Zika Virus Entry
419      Receptor in Neural Stem Cells. Cell stem cell 18: 591-596.

420  33. Tabata T, Petitt M, Puerta-Guardo H, Michlmayr D, Wang C, et al. (2016) Zika Virus
421      Targets Different Primary Human Placental Cells, Suggesting Two Routes for
422      Vertical Transmission. Cell host & microbe 20: 155-166.
423  34. Savidis G, McDougall William M, Meraner P, Perreira Jill M, Portmann Jocelyn M,
424      et al. (2016) Identification of Zika Virus and Dengue Virus Dependency Factors
425      using Functional Genomics. Cell reports 16: 232-246.
426  35. Welsch S, Miller S, Romero-Brey I, Merz A, Bleck CK, et al. (2009) Composition
427      and three-dimensional architecture of the dengue virus replication and assembly
428      sites. Cell host & microbe 5: 365-375.
429  36. Zhang R, Miner JJ, Gorman MJ, Rausch K, Ramage H, et al. (2016) A CRISPR
430      screen defines a signal peptide processing pathway required by flaviviruses.
431      Nature 535: 164-168.
432  37. Prisant N, Bujan L, Benichou H, Hayot PH, Pavili L, et al. (2016) Zika virus in the
433      female genital tract. The Lancet Infectious diseases.
434  38. Foy BD, Kobylinski KC, Chilson Foy JL, Blitvich BJ, Travassos da Rosa A, et al.
435      (2011) Probable non-vector-borne transmission of Zika virus, Colorado, USA.
436      Emerging infectious diseases 17: 880-882.
437  39. Wira CR, Rodriguez-Garcia M, Patel MV (2015) The role of sex hormones in
438      immune protection of the female reproductive tract. Nature reviews Immunology
439      15: 217-230.
440  40. Alexandre KB, Mufhandu HT, London GM, Chakauya E, Khati M (2016) Progress
441      and Perspectives on HIV-1 microbicide development. Virology 497: 69-80.
442
443
444

445    **SUPPORTING INFORMATION CAPTIONS**

446    **Fig S1**. Infection of HESC with Puerto Rico 2015 and Thailand 2013 ZIKV strains.

447    **Fig S2**. Time course of bioactive IFN-β release in response to ZIKV in T-HESC and dT-

448    HESC.

449    **Table S1**. Primers used in the study
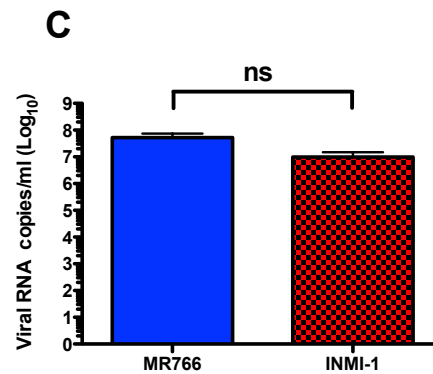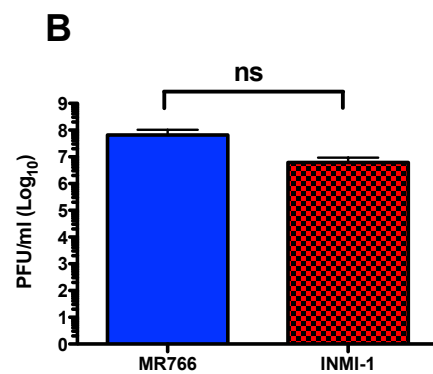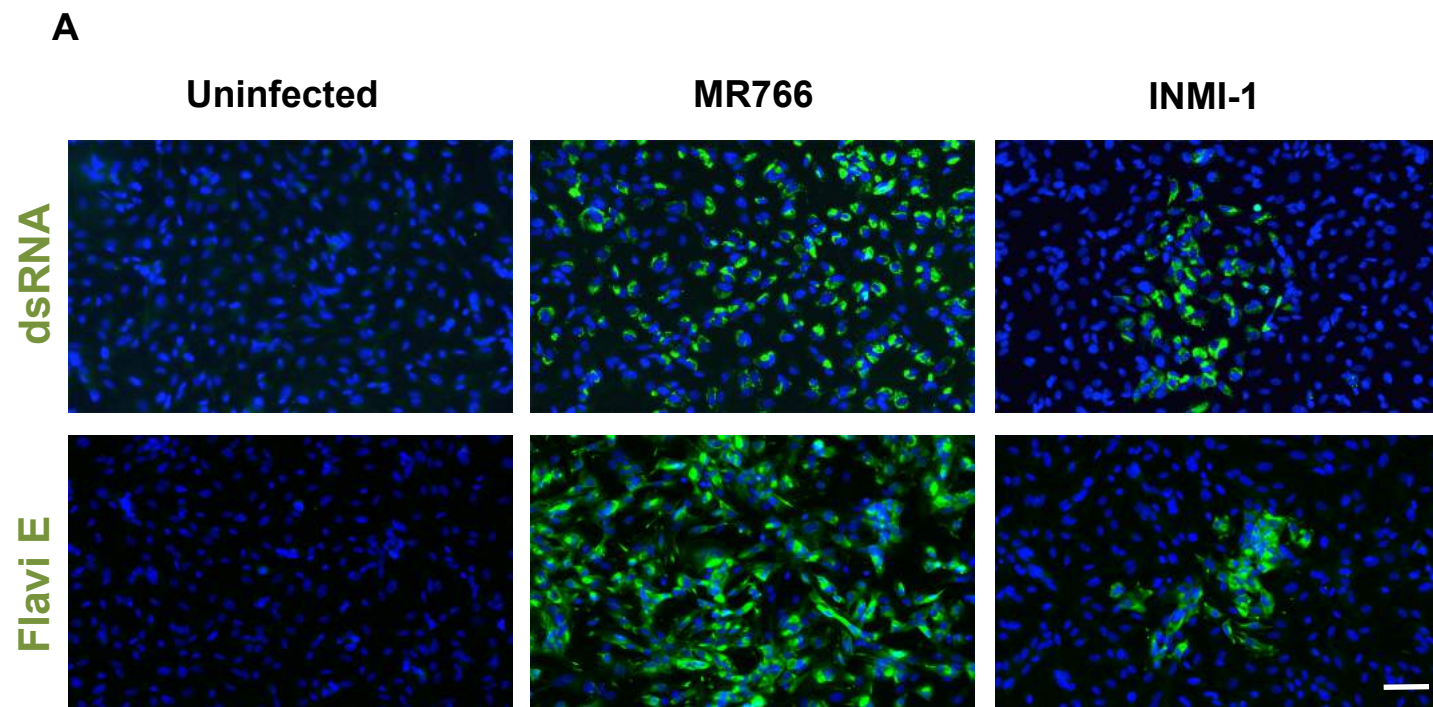
450    Supporting experimental procedures

# Figure 1

**A**



**B**



**C**

**Figure 1. Primary HESC are permissive to ZIKV productive infection. (A)** Immunostaining for dsRNA and Flavi E of primary HESC infected with MR766 and INMI-1 ZIKV strains 72 h post-infection; Hoechst was used to stain nuclei. Scale bar: 20 μm. **(B)** Viral titers in HESC supernatant harvested 3 days after infection as determined by a PFA in VERO cells. Mean ± SEM of 8 independent donors in duplicate cultures. Ns, not significant. **(C)** Viral RNA quantification in HESC supernatants harvested 3 days post-infection as determined by ddPCR. Mean ± SEM of 8 independent donors.
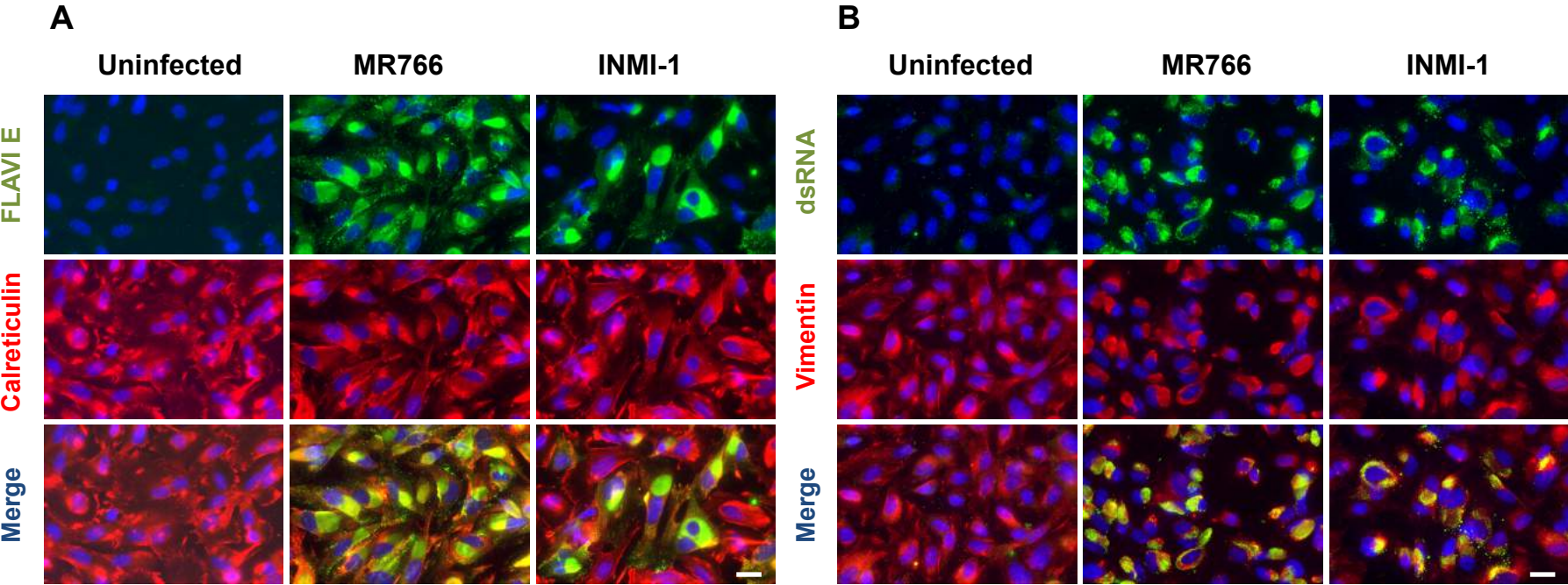
# Figure 2

**Figure 2. Co-localization of ZIKV with calreticulin and vimentin in HESC**. **(A)** Double immunostaining for Flavi E and calreticulin in primary HESC either uninfected or infected with MR766 and INMI-1 at 72 h post-infection; Hoechst was used to stain nuclei. Scale bar: 10 µm. **(B)** Double immunostaining for dsRNA and vimentin in primary HESC either uninfected or infected with MR766 and INMI-1 at 72h post-infection; Hoechst was used to stain nuclei. Scale bar: 10 µm.
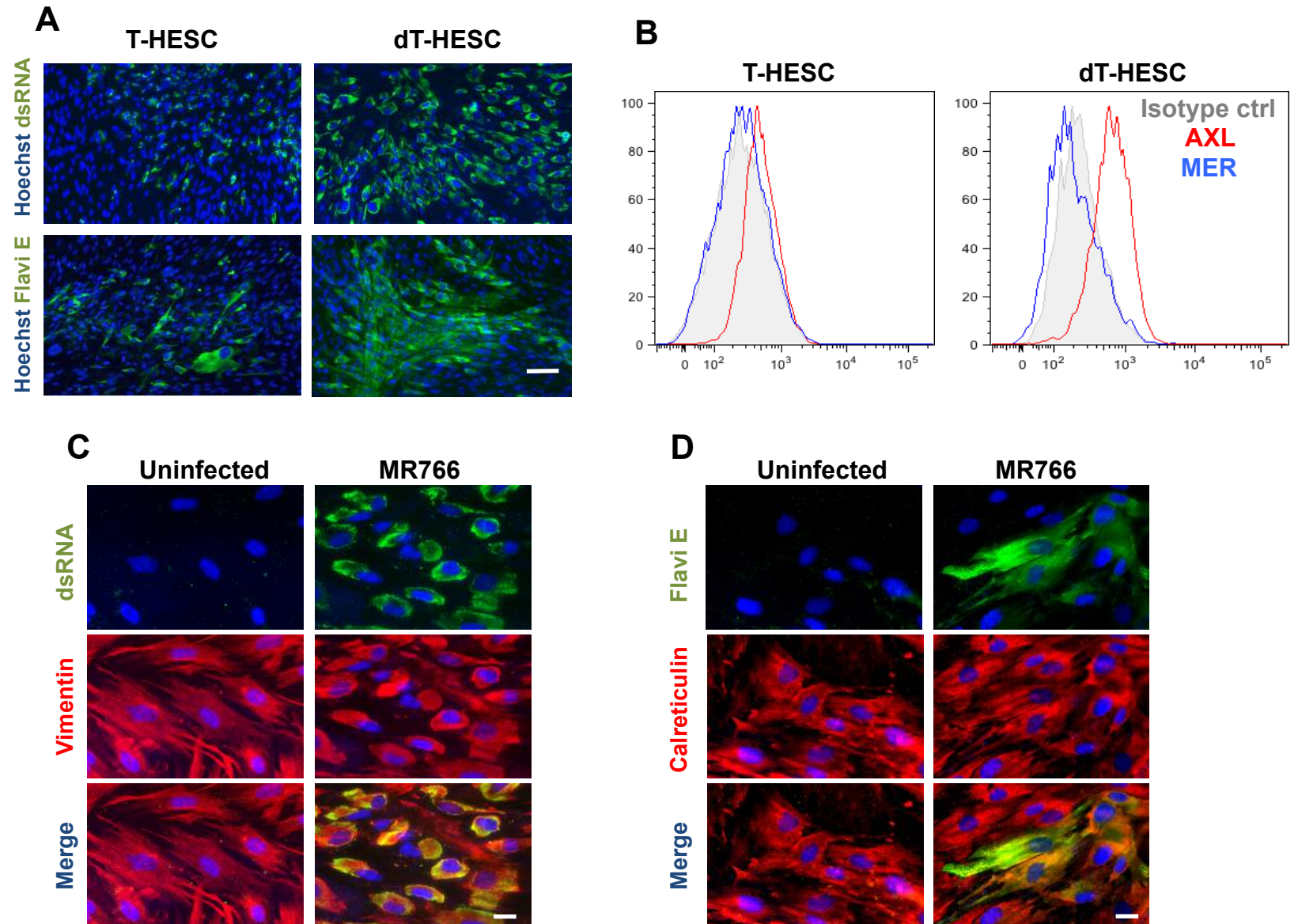
# Figure 3

**Fig 3. ZIKV infection of unstimulated and decidualized T-HESC cell line. (A)** T-HESC (left) and decidualized (d)T-HESC (right) were stained with anti-dsRNA or Flavi E mAbs whereas the nuclei were stained with Hoechst. Scale bar: 20 μm. **(B)** Surface expression of AXL (red) and MER (blue) in T-HESC (left) and dT-HESC (right) was determined by flow cytometry. The histograms of one experiment representative of 3 independently performed are shown. Double immunostaining for Flavi E and calreticulin **(C)** or vimentin **(D)** in T-HESC (left) and dT-HESC (right) either uninfected or infected with MR766 at 72 h post-infection; Hoechst was used to stain nuclei. Scale bar: 10 μm.
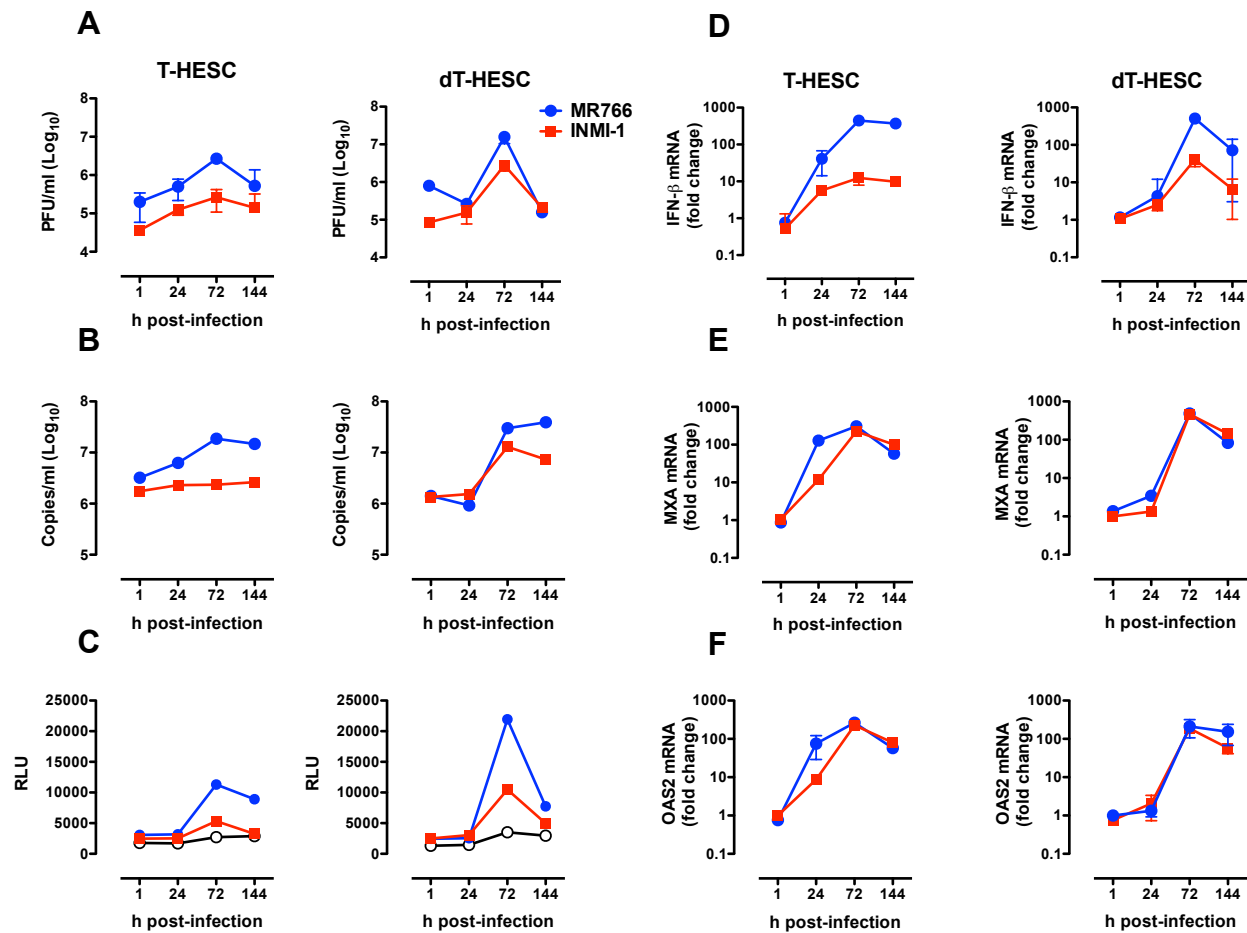
# Figure 4

**Figure 4. ZIKV replication, cytopathicity and induction of IFN-b and ISG expression in T-HESC and dT-HESC.** Kinetics of virus replication in T-HESC (left) and dT-HESC (right) were measured by retrotitration of culture supernatants in Vero cells by PFA (**A**) and by ddPCR (**B**). (**C**) Kinetics of cell death were measured by the activity of cell-associated adenylate kinase released in cell culture supernatants. Open circles indicate uninfected cells. Time course of IFN-β mRNA (**D**), MXA (**E**) and OAS2 (**F**) expression in T-HESC (left) and dT-HESC (right) quantified by RT-qPCR. The results are expressed as the fold induction of transcripts in ZIKV-infected cells relative to those of uninfected cells. The results of one experiment representative of 3 independently conducted are shown.